Scattering Theory of Thermal and Bipolar Thermoelectric Diodes

José Balduque[1,2] and Rafael Sánchez[1,2,3]
[1]Departamento de Física Teórica de la Materia Condensada, Universidad Autónoma de Madrid, 28049 Madrid, Spain
[2]Condensed Matter Physics Center (IFIMAC), Universidad Autónoma de Madrid, 28049 Madrid, Spain
[3]Instituto Nicolás Cabrera (INC), Universidad Autónoma de Madrid, 28049 Madrid, Spain

(Received 31 July 2024; accepted 2 April 2025; published 7 May 2025)

We investigate the minimal requirements that induce a nonreciprocal response to temperature differences in a mesoscopic electronic conductor. We identify two distinct mechanisms involved in electron-electron interactions, namely inelastic scattering and screening, that locally affect the internal properties of the device, leading to thermal and thermoelectric rectification effects in the absence of inversion symmetry. We propose resonant tunneling samples to efficiently exploit these effects, and find configurations acting as bipolar thermoelectric diodes whose current flows in the same direction irrespective of the sign of the temperature difference, a case of antireciprocity.

DOI: 10.1103/PhysRevLett.134.186301

Introduction—Macroscopic materials and devices typically show a linear response to temperature differences [1], with deviations being described recently in extended low-dimensional systems [2–5]. This regime is governed by the principle of microreversibility, that has profound consequences such as Onsager reciprocity relations [6]. This means that reversing the temperature differences applied to the two terminals of a conductor changes the sign of the charge and heat currents, but not their magnitude. In the quantum regime, and in the absence of strong interactions, these properties can be derived from the scattering matrix defining the conductor close to equilibrium [7]. Nanoscale devices [8] that avoid these constraints are strongly demanded to define diodes whose conduction properties are sensitive to nonequilibrium states on chip (due to, e.g., undesired hot spots or leakage heat flows): nonreciprocal currents are different in the forward (F) and backward (B) configurations, when a temperature increase ΔT holds either on the left or on the right terminal; see Fig. 1(a). Most proposals so far are based on specific realizations dominated by electron-electron interactions [9–16], with so far very few experiments detecting nonreciprocal thermal or thermoelectric responses to temperature differences [17–19]. Some other works can be interpreted in terms of noninteracting electrons, however, requiring the coupling to additional degrees of freedom (phonons, photons) [20–29], a quantum detector [30,31], or a third terminal [16,32–35], all involving heat being dissipated elsewhere rather than rectified. Photonic thermal rectification in quantum information systems is also intensively investigated [36–47]. However, an overall description of the microscopic origin of temperature-driven electronic diodes is missing that is not restricted to near equilibrium situations [48–52].

Here, we investigate the onset of temperature-driven diode effects by exploring the geometric and dynamic consequences of reduced dimensionality conductors: on one hand, they have a low capacitance [53]; on the other hand, their size can be comparable to the carrier thermalization length [54]. Both features emphasize the importance of electron-electron interactions: charge accumulation in the conductor alters the internal potential, while the momentum transfer involved in the Coulomb interaction results in inelastic scattering, phase randomization, and thermalization within the nanostructure. Importantly, we will not require any external environment such that energy is conserved in the conductor: at low temperatures, the electron-phonon coupling is negligible. The key aspect is that the state of the quantum system is sensitive to the temperature distribution in the two terminals, for which one

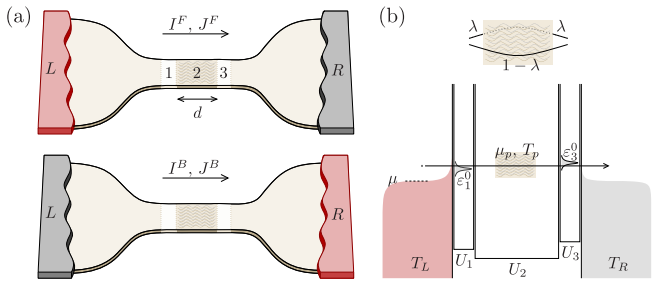

FIG. 1. Scheme of a temperature-induced diode. (a) It consists on three regions: 1 and 3, where transport is elastic, and 2, where electrons may thermalize. Particle (I) and heat (J) currents responding to differences in the temperature T_j of terminals $j = L, R$ are sensitive to the forward (F) or backward (B) configuration where temperature is increased in terminal L or R. (b) Scheme of a probe modeling thermalization in region 2 that absorbs (reflects) electrons with probability λ ($1-\lambda$), and (c) of a configuration where regions 1 and 2 are tunnel junctions with resonances at energy ε_α^0 with respect to the corresponding band bottom, U_α.

additionally needs to impose broken (left-right) inversion symmetry.

To keep the discussion simple, we use a scattering theory based description, which is well established close to the linear regime as long as electron-electron interactions can be treated in a mean field level [55–57]. Nontrivial extensions of the theory are needed that account for nonlinearities [58] (relating charge accumulation in the conductor to rectification and diode effects [57]) and inelastic scattering [59–61] (treated phenomenologically). For this, we consider the configuration sketched in Fig. 1(a): thermoelectric particle, I, and heat, J, currents through a quantum conductor are due to temperature differences between terminals L and R [62,63]. The conductor is partitioned in three, with regions $\alpha = 1$, 3 sandwiching region 2, of length d, where electrons are ballistic but have a finite probability λ to thermalize. Despite its simplicity, this model can be applied to a wide range of configurations, including quantum wires [64–68], molecular junctions [69,70], chaotic cavities [71] (which enhance thermalization [72]), or quantum dots [73]. Remarkably, it not only allows us to identify the relevant mechanisms for thermoelectric and thermal rectification, it also predicts an antireciprocal response: a bipolar thermoelectric effect in particular configurations for which particles flow in the same direction independently of which terminal is hot. We discuss how this effect depends on the breaking of the microreversibility principle for the different involved mechanisms.

Scattering theory—The transport properties of a single-channel conductor are described by its scattering matrix, $\mathcal{S}(E)$. With the current density in terminal j,

$$\mathcal{I}_j(E) = \frac{2}{h}\sum_k |\mathcal{S}_{kj}(E)|^2 [f_j(E) - f_k(E)], \tag{1}$$

one writes the particle $I_j = \int dE \mathcal{I}_j(E)$ and heat currents $J_j = \int dE(E-\mu_j)\mathcal{I}_j(E)$ [62], where $f_j(E) = 1/\{1 + \exp[(E-\mu_j)/k_B T_j]\}$ is the Fermi function of terminal j at temperature T_j and electrochemical potential μ_j, h, and k_B are the Planck and Boltzmann constants, and the factor 2 accounts for spin degeneracy [74]. We consider the scattering region to have a piecewise uniform band bottom $\mathbf{U} \equiv \{U_\alpha\}$, which will influence the shape of $\mathcal{S}(E) = \mathcal{S}(E, \mathbf{U})$. For later convenience, we split them into equilibrium (including the effect of gate voltages) and nonequilibrium contributions: $U_\alpha = U_\alpha^{\mathrm{eq}} + U_\alpha^{\mathrm{neq}}$. Note that since the particle flow relies on the thermoelectric effect, $\mathcal{S}(E)$ needs to be energy dependent [54].

We are interested in two-terminal conductors, with $j = L$, R, only driven by a temperature difference ΔT applied either to L (the forward) or to R (the backward case), with the opposite terminal being at temperature T, and both having the same electrochemical potential, $\mu = \mu_L = \mu_R$. The diode effect appears when the particle or heat currents, $X^i(T_L, T_R) = I_L^i, J_L^i$ $(i = F,\ B)$, are nonreciprocal, i.e., $X^F \neq -X^B$, with $X^F \equiv X(T + \Delta T, T)$ and $X^B \equiv X(T, T + \Delta T)$. We quantify this effect with the thermoelectric, $\mathcal{R}_I$, and thermal, $\mathcal{R}_J$, rectification coefficients [75],

$$\mathcal{R}_X = \frac{X^F + X^B}{|X^F| + |X^B|}, \tag{2}$$

which saturate to ± 1 only when one of the currents is zero (perfect diode) or when both have the same sign. In the latest case, the diode is bipolar.

We readily see that assuming fully noninteracting particles, for which the scattering matrix is independent of the reservoir temperatures, both currents X^i are antisymmetric under the exchange $T_L \leftrightarrow T_R$ [cf. Eq. (1) for $j = L$ and $k = R$], resulting in no rectification, $\mathcal{R}_X = 0$. A diode hence needs that the nanostructure is sensitive to the terminal temperatures.

In what follows, we explore the role of interactions as a requisite for thermal and thermoelectric rectification. We consider two separate ways in which interactions can modify the electron propagation through the system, namely inelastic scattering and screening effects.

Inelastic scattering—When two electrons interact, they exchange momentum, which involves that they change their energies and randomize their kinetic phases, limiting both the elastic and phase-coherent transport implicit in Eq. (1), while conserving their total energy. In scattering theory, this effect is routinely described phenomenologically by introducing a fictitious probe [60,61,76–80] that absorbs electrons with probability λ [81] and reinjects them with a random phase and thermalized with a distribution $f_p(E)$ whose electrochemical potential, μ_p, and temperature, T_p, are determined by imposing that the probe injects no particle and no heat currents on average, $I_p = J_p = 0$. Intuitively λ relates the inelastic scattering length l_{inel} to the typical size of the system, l: $\lambda \ll 1$ when $l_{\mathrm{inel}} \gg l$, and $\lambda \approx 1$ in the opposite limit. Quantum Hall realizations relate λ to the transmission of a quantum point contact [82]. Trajectories involving the probe do not obey microreversibility. On a microscopic description of the particular models, there may be small deviations from a Fermi distribution function, especially at very low temperatures and far from equilibrium [83], that are not relevant for our discussion here. Our thermalization probe, sketched in Fig. 1(b), is hence formally equivalent to a thermometer [84–87] and useful to discuss thermalization in hot-carrier solar cells [88], broken-time-reversal-induced electrical diodes [79], and correlations in edge channels [89]. Note that while the flow of heat will be determined by $T_L - T_R$, the particle currents may be affected by the competition of the thermoelectric effect and the developed $\mu_p - \mu$.

The rectification properties of thermalization is proven analytically by considering a simple configuration in

which all electrons in the conductor are thermalized ($\lambda = 1$), with region 3 being transparent (so $\mathcal{S}_{pR} = \mathbb{1}$) and region 1 being a barrier with transmission probability $\mathcal{T}(E) = |\mathcal{S}_{pL}(E)|^2$; cf. Fig. 1(a). In the limit $\mu - U_\alpha \gg k_B T$, the contributions of terminal R to the currents into the probe are given by $\int dE[f_R(E) - f_p(E)] = \mu - \mu_p$ and $\int dE E[f_R(E) - f_p(E)] = \pi^2(T_R^2 - T_p^2)/6$. The other contribution to the probe currents coincides with X^i, which are then determined by the probe conditions

$$I^i = \frac{2}{h}(\mu_{p,i} - \mu) \quad \text{and} \quad J^i = \frac{\pi^2}{3h}(T_{p,i}^2 - T_{R,i}^2), \tag{3}$$

with $T_{R,F} = T$ and $T_{R,B} = T + \Delta T$. The spatial asymmetry here is due to the position of the thermalization region with respect to the thermoelectric element, which is enough to have $T_p^F \neq T_p^B$. A thermoelectric diode needs that $\mathcal{T}(E)$ breaks electron-hole symmetry, so region 1 has a finite electric response giving $\mu_p^F \neq \mu_p^B$ [81].

We now consider a more specific setup, sketched in Fig. 1(c), that allows us to control the degree of asymmetry experimentally [73,90]. We choose the scattering regions 1 and 3 to be resonant-tunneling barriers (RTBs), known efficient thermoelectric devices [91–95]. We model them by Breit-Wigner resonances [96] with energy ε_α^0 and inverse lifetime $\Gamma_\alpha/\hbar$ [61] and transmission amplitude [81]

$$\tau_\alpha = \frac{-i\Gamma_\alpha}{E - \varepsilon_\alpha^0 - U_\alpha + i\Gamma_\alpha}, \qquad (\alpha = 1, 3). \tag{4}$$

For simplicity, we assume $\Gamma_1 = \Gamma_3 \equiv \Gamma$, and a totally coupled probe ($\lambda = 1$) so direct elastic transport between terminals L and R is suppressed, a configuration of experimental relevance [73,97,98]. We incorporate U_α^{eq}, which allows us to control the system asymmetry via gate voltages, in the resonance energies $\varepsilon_\alpha = \varepsilon_\alpha^0 + U_\alpha^{\mathrm{eq}}$, and neglect U_α^{neq} here.

The resulting currents and rectification coefficients are plotted in Figs. 2(a)–2(d) by tuning the resonance energies of the barriers. As expected, broken inversion symmetry when $\varepsilon_1 \neq \varepsilon_3$ results in finite $\mathcal{R}_I$ and $\mathcal{R}_J$, while $\mathcal{R}_X = 0$ for symmetric cases with $\varepsilon_1 = \varepsilon_3$.

The antisymmetric configuration with $\varepsilon_1 - \mu = \mu - \varepsilon_3$ is particularly interesting: while inversion symmetry is maximally broken, it respects electron-hole symmetry in equilibrium. The two RTBs have opposite thermoelectric contributions resulting in a vanishing linear response for particles [see Fig. 2(a)]: writing $I^i = \sum_n L^{(n),i}\Delta T^n$, we get $L^{(1),i} = 0$, with the probe developing a temperature $T_p^F = T_p^B = T + \Delta T/2$ and electrochemical potentials of opposite sign in F and B, $\mu_p^F + \mu_p^B = 2\mu$ [81]. This affects the nonlinear terms (of order $\geq \Delta T^2$), making I^F and I^B vanish at different points (determined by the corresponding μ_p and T_p) when, e.g., tuning ε_1; see inset in Fig. 2(a). At the

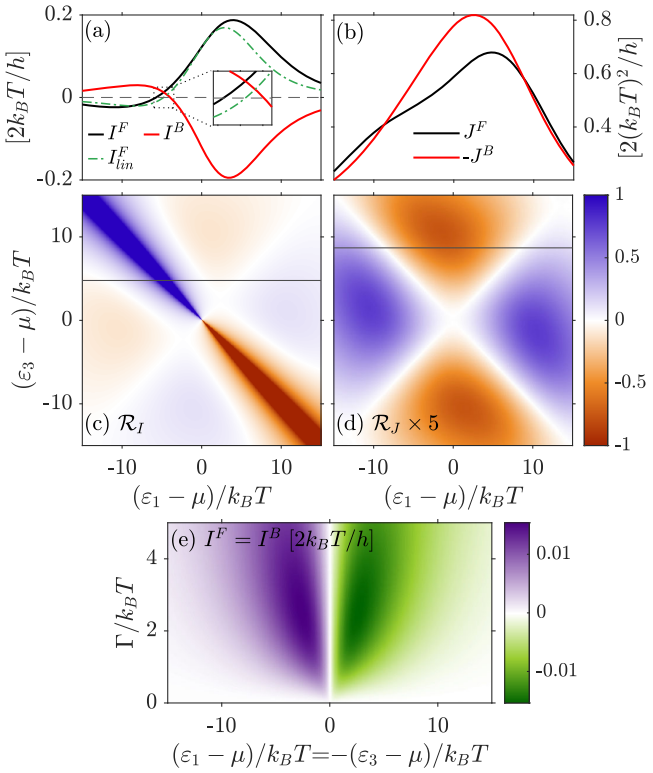

FIG. 2. Thermalization diode. Forward and backward (a) particle and (b) heat currents as functions of ε_1 tuned along $(\varepsilon_3 - \mu)/k_BT = 4.8$ and 8.7, respectively, indicated by black lines in (c) and (d). The latter panels show the thermoelectric and heat rectification coefficients as functions of both resonances. The thermalization probe is fully coupled ($\lambda = 1$), and $\mu \gg U_\alpha$, avoiding band bottom effects. The linear response current, $I_{\mathrm{lin}}^F = L^{(1)F}\Delta T$, is shown for comparison in (a). Parameters: $\Gamma = 3k_BT$, $\mu = 40k_BT$, and $\Delta T/T = 1$.

vanishing points, the current flows only in one of the configurations, as an ideal thermoelectric diode with $\mathcal{R}_I = 1$ (working, however, only for a particular ΔT). Most remarkably, between vanishing points, the current flows in the same direction irrespective of which terminal is hot. This is what we call a bipolar thermoelectric (or antireciprocal) diode. Furthermore, at the antisymmetric condition $\varepsilon_1 + \varepsilon_3 = 2\mu$, the problem symmetry imposes $I^F = I^B$ [81], with their sign being tunable and maximal for widths $\Gamma \approx 2k_BT$ (consistent with similar configurations [99–101]); see Fig. 2(e).

Differently, the heat currents do not change sign (as imposed by the second law) [see Fig. 2(b)], which avoids a bipolar thermal diode if $\mu_j = \mu$. We find $\mathcal{R}_J \sim 15\%$, cf. Fig. 2(d), and $\mathcal{R}_J = 0$ for $(\varepsilon_1 - \mu) = \pm(\varepsilon_3 - \mu)$, where both RTBs conduct heat equally.

Screening effects—The injection of a charge current is able to alter the potential landscape of the conductor via charge accumulation and screening effects in the nearby gates defining the scattering regions [102,103]. This consequence of electron-electron interaction is in fact

needed to ensure gauge invariance in nonlinear scenarios [58]. Deviations from the linear regime leading to finite thermal and thermoelectric rectification have been discussed in the weakly interacting regime [48,50–52].

We again test this mechanism in the setup of Fig. 1(c), now with $\lambda = 0$, so that transport between terminals is fully elastic. Then, an important contribution will be the internal reflections in region 2, leading to Fabry-Perot interferences. Scattering at the barriers is again given by Eq. (4). Screening affects the internal electrostatic energies, $\mathbf{U}$, by developing finite $U_\alpha^{\rm neq}(T_L, T_R)$, and modifies the scattering matrix of the whole system, $\mathcal{S}(E, \mathbf{U})$ [81]. The energies $\mathbf{U}$ are linked by

$$\delta q_\alpha = \sum_{\beta=1,2,3\neq\alpha} C_{\alpha\beta}(U_\beta - U_\alpha)/(-e), \tag{5}$$

where δq_α is the injected charge in region α with respect to the equilibrium scenario, and $C_{\alpha\beta}$ the geometric capacitance between regions α and β, treated here as a parameter. The excess charge can be calculated with the aid of the partial local densities of states of the system, or injectivities [103],

$$\nu_{j\alpha}(E, \mathbf{U}) = \frac{i}{4\pi}\sum_k \left[\mathcal{S}_{kj}^\dagger \frac{\delta \mathcal{S}_{kj}}{\delta U_\alpha} - \frac{\delta \mathcal{S}_{kj}^\dagger}{\delta U_\alpha}\mathcal{S}_{kj}\right], \tag{6}$$

defining the overlap of waves in region α with states injected at terminal j, via

$$\frac{\delta q_\alpha}{-e} = \int dE \sum_j [\nu_{j\alpha}(E, \mathbf{U}) f_j(E) - \nu_{j\alpha}^{\rm eq} f_{\rm eq}(E)], \tag{7}$$

with $\nu_{j\alpha}^{\rm eq}$ and $f_{\rm eq}(E)$ evaluated at equilibrium. Note that we do not assume a weak deviation from equilibrium [104].

We show in Figs. 3(a) and 3(b) the resulting currents in the limit $C_{\alpha\beta} \to 0$ for small conductors. The thermoelectric response shows an oscillating behavior, with sign changes close to the crossings of the barrier resonances by the chemical potential, and at the crossing of the two resonances. As $\mathbf{U}$ depends on the temperature distribution, these crossings occur at different points in F and B, again resulting in regions with $\mathcal{R}_I = 1$; see Fig. 3(c). The heat currents do not change sign, finding wide regions with strong rectification ($\mathcal{R}_J \sim 0.2$) close to the resonance condition $\varepsilon_1 \approx \varepsilon_3$; see Fig. 3(d).

Screening hence also induces a bipolar thermoelectric diode, in this case respecting microreversibility: $|\mathcal{S}_{LR}(E, \mathbf{U})|^2 = |\mathcal{S}_{RL}(E, \mathbf{U})|^2 = \mathcal{T}(E)$. To further understand this mechanism, let us concentrate on the particular configuration marked by $\star$ in Fig. 3(a), where $I^F = I^B$. There, both resonances are over the chemical potential and slightly detuned, $\varepsilon_3 > \varepsilon_1 > \mu$. The transmission probability $\mathcal{T}(E)$ [see Fig. 3(e)] shows two main features with opposite thermoelectric contributions: a wide double peak around $\varepsilon_1, \varepsilon_3 > \mu$, and a sharp peak at $E < \mu$ due to the

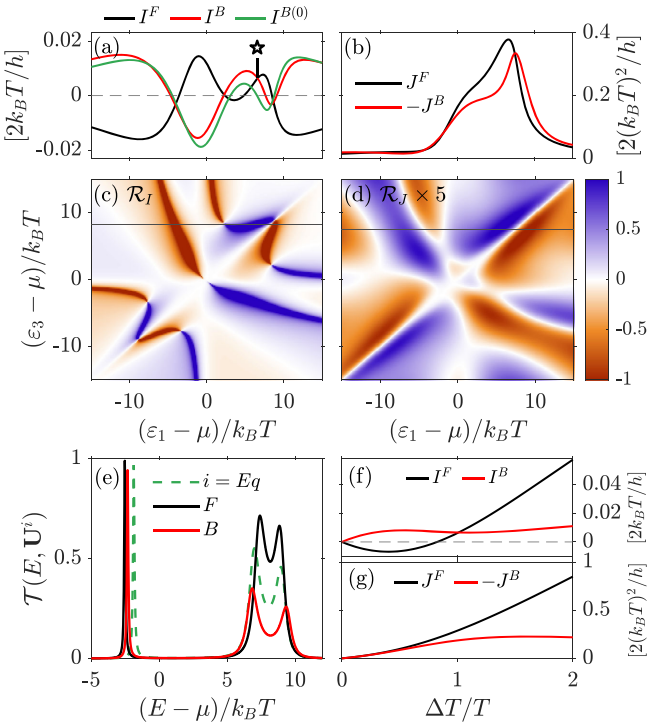

FIG. 3. Rectification by screening. (a) Particle and (b) heat currents as functions of ε_1, for fixed $(\varepsilon_3 - \mu)/k_{\rm B}T = 8.2$ and 7.5 as marked by black lines in (c) and (d), respectively. The latter show the dependence of $\mathcal{R}_I$ and $\mathcal{R}_J$ with gating the RTBs. The green curve in (a) shows the current obtained by imposing the equilibrium transmission probability, for comparison. (e) Transmission probability in equilibrium and in the F and B configurations at the point marked by $\star$ in (a), for which the temperature dependence of the charge and heat currents are shown in (f) and (g). Parameters: $\lambda = 0$, $d = 2h/\sqrt{8mk_{\rm B}T}$, $\Gamma = k_{\rm B}T$, $\mu = 40k_{\rm B}T$, $\Delta T/T = 1$.

Fabry-Perot interference in $\alpha = 2$. Note that $\mathcal{T}(E \approx \mu)$ is flat, which suppresses the linear term ($L^{(1)} \propto \partial\mathcal{T}/\partial E$) according to the Mott formula [54]. In F, increasing T_L increases δq_1 and hence U_1, bringing the two Breit-Wigner resonances closer and resulting in a sharper and higher double peak at positive energies; see Fig. 3(e). Oppositely, the corresponding increase of U_3 in B separates the two resonances, making the double peak wider and lower, i.e., reducing its contribution to I^B. Eventually, the opposite contribution of the Fabry-Perot peak at negative energies dominates, inducing I^B to change sign [81]. This bipolar diode is hence induced not only by screening but also by quantum interference.

The bipolar effect persists for higher ΔT, cf. Fig. 3(f), and the thermal diode is robust: one polarity exhibits vanishing and even negative thermal differential conductance for large ΔT [81]; see Fig. 3(g). We attribute this effect to the same mechanism discussed above.

Mixed regime—To confirm the quantum interference origin of the screening-induced bipolar thermoelectric

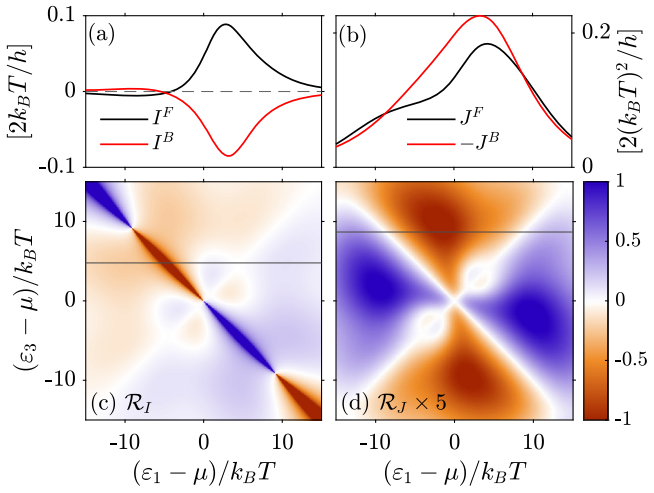

FIG. 4. Mixed configuration. Same as Figs. 3(a)–3(d) for $\lambda = 1$.

diode, we compute a mixed configuration where screening coexists with thermalization, cf. Fig. 4. For $\lambda = 1$, the probe avoids any Fabry-Perot interference in region 2. Hence screening only contributes to shift U_1 and U_3. By comparing Figs. 2, 3, and 4 we see that the currents are indeed dominated by thermalization, and the interference-induced off-diagonal features in $\mathcal{R}_I$ are strongly suppressed [81]. Still, we find a thermalization-induced bipolar effect around $\varepsilon_1 - \mu = \mu - \varepsilon_3$.

Conclusions—We have provided a fully quantum mechanical description of temperature-induced mesoscopic diodes by considering interaction-induced thermalization and screening affecting elastic transport (strongly correlated effects like Coulomb blockade, however, are not covered [105]). With this we find diode effects both for particle and thermal currents. Remarkably, we find an *antireciprocal* response in the form of a bipolar thermoelectric effect caused by both thermalization and screening-controlled quantum interference in ballistic resonant tunneling configurations. While the fully thermalized case can be interpreted in terms of locally reversing currents between three regions (the reservoirs and the internal thermalization region) at different thermal configurations, the fully coherent case exploits nonequilibrium states and quantum interference to achieve antireciprocity while maintaining microreversibility. In both cases, it occurs when sharp spectral features with opposite but similar in magnitude thermoelectric contributions depend differently on the local reaction of the conductor to the nonequilibrium situation. We find measurable currents of a few nA at mK temperatures in state of the art configurations [73,98].

Related effects have been predicted before, however, requiring dissipation [26,30,31] or multiterminal configurations [33–35]. Differently, our treatment imposes particle and energy conservation in the two-terminal diode. Our results add to other recently found bipolar nonlinear thermoelectric functionalities in superconducting junctions [106–108] (based on spontaneous symmetry breaking mechanisms), contributing to set the base for thermally driven on-chip devices.

Acknowledgments—We thank Y. Tokura and A. Braggio for useful discussions. We acknowledge funding from the Spanish Ministerio de Ciencia e Innovación via Grant No. PID2019–110125GB-I00 and No. PID2022-142911NB-I00, and through the "María de Maeztu" Programme for Units of Excellence in R&D CEX2023-001316-M.

[1] N. W. Ashcroft and N. D. Mermin, *Solid State Physics* (Saunders College Publishing, Orlando, USA, 1976).
[2] Y. D. Wang, Z.-G. Zhu, and G. Su, Quantum theory of nonlinear thermal response, Phys. Rev. B **106**, 035148 (2022).
[3] T. Yamaguchi, K. Nakazawa, and A. Yamakage, Microscopic theory of nonlinear Hall effect induced by electric field and temperature gradient, Phys. Rev. B **109**, 205117 (2024).
[4] H. Arisawa, Y. Fujimoto, T. Kikkawa, and E. Saitoh, Observation of nonlinear thermoelectric effect in MoGe/Y3Fe5O12, Nat. Commun. **15**, 6912 (2024).
[5] P. Chatterjee and P. Dutta, Quasiparticles-mediated thermal diode effect in Weyl Josephson junctions, New J. Phys. **26**, 073035 (2024).
[6] L. Onsager, Reciprocal relations in irreversible processes. I, Phys. Rev. **37**, 405 (1931); Reciprocal relations in irreversible processes. II, Phys. Rev. **38**, 2265 (1931).
[7] P. Jacquod, R. S. Whitney, J. Meair, and M. Büttiker, Onsager relations in coupled electric, thermoelectric, and spin transport: The tenfold way, Phys. Rev. B **86**, 155118 (2012).
[8] J. P. Pekola and B. Karimi, Colloquium: Quantum heat transport in condensed matter systems, Rev. Mod. Phys. **93**, 041001 (2021).
[9] C. Xue-Ou, D. Bing, and L. Xiao-Lin, Thermal rectification effect of an interacting quantum dot, Chin. Phys. Lett. **25**, 3032 (2008).
[10] D. M.-T. Kuo and Y.-c. Chang, Thermoelectric and thermal rectification properties of quantum dot junctions, Phys. Rev. B **81**, 205321 (2010).
[11] T. Ruokola and T. Ojanen, Single-electron heat diode: Asymmetric heat transport between electronic reservoirs through Coulomb islands, Phys. Rev. B **83**, 241404(R) (2011).
[12] M. A. Sierra and D. Sánchez, Strongly nonlinear thermovoltage and heat dissipation in interacting quantum dots, Phys. Rev. B **90**, 115313 (2014).
[13] M. A. Sierra and D. Sánchez, Nonlinear heat conduction in coulomb-blockaded quantum dots, Mater. Today **2**, 483 (2015).
[14] L. Vannucci, F. Ronetti, G. Dolcetto, M. Carrega, and M. Sassetti, Interference-induced thermoelectric switching and heat rectification in quantum Hall junctions, Phys. Rev. B **92**, 075446 (2015).

[15] A. Marcos-Vicioso, C. López-Jurado, M. Ruiz-Garcia, and R. Sánchez, Thermal rectification with interacting electronic channels: Exploiting degeneracy, quantum superpositions, and interference, Phys. Rev. B **98**, 035414 (2018).
[16] L. Tesser, B. Bhandari, P. A. Erdman, E. Paladino, R. Fazio, and F. Taddei, Heat rectification through single and coupled quantum dots, New J. Phys. **24**, 035001 (2022).
[17] R. Scheibner, M. König, D. Reuter, A. D. Wieck, C. Gould, H. Buhmann, and L. W. Molenkamp, Quantum dot as thermal rectifier, New J. Phys. **10**, 083016 (2008).
[18] S. F. Svensson, E. A. Hoffmann, N. Nakpathomkun, P. M. Wu, H. Q. Xu, H. A. Nilsson, D. Sánchez, V. Kashcheyevs, and H. Linke, Nonlinear thermovoltage and thermocurrent in quantum dots, New J. Phys. **15**, 105011 (2013).
[19] J. Fast, H. Lundström, S. Dorsch, L. Samuelson, A. Burke, P. Samuelsson, and H. Linke, Geometric symmetry breaking and nonlinearity can increase thermoelectric power, Phys. Rev. Lett. **133**, 116302 (2024).
[20] D. Segal, Single mode heat rectifier: Controlling energy flow between electronic conductors, Phys. Rev. Lett. **100**, 105901 (2008).
[21] M. J. Martínez-Pérez and F. Giazotto, Efficient phase-tunable Josephson thermal rectifier, Appl. Phys. Lett. **102**, 182602 (2013).
[22] M. J. Martínez-Pérez, A. Fornieri, and F. Giazotto, Rectification of electronic heat current by a hybrid thermal diode, Nat. Nanotechnol. **10**, 303 (2015).
[23] J.-H. Jiang, M. Kulkarni, D. Segal, and Y. Imry, Phonon thermoelectric transistors and rectifiers, Phys. Rev. B **92**, 045309 (2015).
[24] G. Rosselló, R. López, and R. Sánchez, Dynamical Coulomb blockade of thermal transport, Phys. Rev. B **95**, 235404 (2017).
[25] G. T. Craven, D. He, and A. Nitzan, Electron-transfer-induced thermal and thermoelectric rectification, Phys. Rev. Lett. **121**, 247704 (2018).
[26] J. Lu, R. Wang, J. Ren, M. Kulkarni, and J.-H. Jiang, Quantum-dot circuit-QED thermoelectric diodes and transistors, Phys. Rev. B **99**, 035129 (2019).
[27] D. Goury and R. Sánchez, Reversible thermal diode and energy harvester with a superconducting quantum interference single-electron transistor, Appl. Phys. Lett. **115**, 092601 (2019).
[28] B. Cao, C. Han, X. Hao, C. Wang, and J. Lu, Impact of quantum coherence on inelastic thermoelectric devices: From diode to transistor, Chin. Phys. Lett. **41**, 077302 (2024).
[29] E. L. Mehring, R. A. Bustos-Marún, and H. L. Calvo, Hysteresis and effective reciprocity breaking due to current-induced forces, Phys. Rev. B **109**, 085418 (2024).
[30] P. Bredol, H. Boschker, D. Braak, and J. Mannhart, Decoherence effects break reciprocity in matter transport, Phys. Rev. B **104**, 115413 (2021).
[31] J. Ferreira, T. Jin, J. Mannhart, T. Giamarchi, and M. Filippone, Transport and nonreciprocity in monitored quantum devices: An exact study, Phys. Rev. Lett. **132**, 136301 (2024).
[32] R. Sánchez, B. Sothmann, and A. N. Jordan, Heat diode and engine based on quantum Hall edge states, New J. Phys. **17**, 075006 (2015).
[33] R. Sánchez, H. Thierschmann, and L. W. Molenkamp, Single-electron thermal devices coupled to a mesoscopic gate, New J. Phys. **19**, 113040 (2017).
[34] G. Fleury, C. Gorini, and R. Sánchez, Scanning probe-induced thermoelectrics in a quantum point contact, Appl. Phys. Lett. **119**, 043101 (2021).
[35] R. Sánchez, C. Gorini, and G. Fleury, Extrinsic thermoelectric response of coherent conductors, Phys. Rev. B **104**, 115430 (2021).
[36] D. Segal and A. Nitzan, Spin-boson thermal rectifier, Phys. Rev. Lett. **94**, 034301 (2005).
[37] T. Ojanen, Selection-rule blockade and rectification in quantum heat transport, Phys. Rev. B **80**, 180301(R) (2009).
[38] F. Fratini, E. Mascarenhas, L. Safari, J.-P. Poizat, D. Valente, A. Auffèves, D. Gerace, and M. F. Santos, Fabry-Perot interferometer with quantum mirrors: Nonlinear light transport and rectification, Phys. Rev. Lett. **113**, 243601 (2014).
[39] G. Schaller, G. G. Giusteri, and G. L. Celardo, Collective couplings: Rectification and supertransmittance, Phys. Rev. E **94**, 032135 (2016).
[40] J. Ordonez-Miranda, Y. Ezzahri, and K. Joulain, Quantum thermal diode based on two interacting spinlike systems under different excitations, Phys. Rev. E **95**, 022128 (2017).
[41] S. Barzanjeh, M. Aquilina, and A. Xuereb, Manipulating the flow of thermal noise in quantum devices, Phys. Rev. Lett. **120**, 060601 (2018).
[42] J. Senior, A. Gubaydullin, B. Karimi, J. T. Peltonen, J. Ankerhold, and J. P. Pekola, Heat rectification via a superconducting artificial atom, Commun. Phys. **3**, 40 (2020).
[43] B. Bhandari, P. A. Erdman, R. Fazio, E. Paladino, and F. Taddei, Thermal rectification through a nonlinear quantum resonator, Phys. Rev. B **103**, 155434 (2021).
[44] A. Iorio, E. Strambini, G. Haack, M. Campisi, and F. Giazotto, Photonic heat rectification in a system of coupled qubits, Phys. Rev. Appl. **15**, 054050 (2021).
[45] R. Upadhyay, D. S. Golubev, Y.-C. Chang, G. Thomas, A. Guthrie, J. T. Peltonen, and J. P. Pekola, Microwave quantum diode, Nat. Commun. **15**, 630 (2024).
[46] K. Poulsen and N. T. Zinner, Heat-based circuits using quantum rectification, Phys. Rev. A **109**, 052223 (2024).
[47] A. L. Yeyati, D. Subero, J. P. Pekola, and R. Sánchez, Photonic heat transport through a Josephson junction in a resistive environment, Phys. Rev. B **110**, L220502 (2024).
[48] D. Sánchez and R. López, Scattering theory of nonlinear thermoelectric transport, Phys. Rev. Lett. **110**, 026804 (2013).
[49] R. S. Whitney, Nonlinear thermoelectricity in point contacts at pinch off: A catastrophe aids cooling, Phys. Rev. B **88**, 064302 (2013).
[50] R. S. Whitney, Thermodynamic and quantum bounds on nonlinear dc thermoelectric transport, Phys. Rev. B **87**, 115404 (2013).
[51] J. Meair and P. Jacquod, Scattering theory of nonlinear thermoelectricity in quantum coherent conductors, J. Phys. Condens. Matter **25**, 082201 (2013).

[52] R. López and D. Sánchez, Nonlinear heat transport in mesoscopic conductors: Rectification, Peltier effect, and Wiedemann-Franz law, Phys. Rev. B **88**, 045129 (2013).
[53] T. Ihn, *Semiconductor Nanostructures: Quantum States and Electronic Transport* (Oxford University Press, Oxford, 2009).
[54] G. Benenti, G. Casati, K. Saito, and R. S. Whitney, Fundamental aspects of steady-state conversion of heat to work at the nanoscale, Phys. Rep. **694**, 1 (2017).
[55] R. Landauer, spatial variation of currents and fields due to localized scatterers in metallic conduction, IBM J. Res. Dev. **1**, 223 (1957).
[56] R. Landauer, Conductance determined by transmission: Probes and quantised constriction resistance, J. Phys. Condens. Matter **1**, 8099 (1989).
[57] M. Büttiker and T. Christen, Admittance and nonlinear transport in quantum wires, point contacts, and resonant tunneling barriers, in *Mesoscopic Electron Transport* (Springer, Dordrecht, The Netherlands, 1997), pp. 259–289.
[58] T. Christen and M. Büttiker, Gauge-invariant nonlinear electric transport in mesoscopic, Europhys. Lett. **35**, 523 (1996).
[59] H.-L. Engquist and P. W. Anderson, Definition and measurement of the electrical and thermal resistances, Phys. Rev. B **24**, 1151(R) (1981).
[60] M. Büttiker, Role of quantum coherence in series resistors, Phys. Rev. B **33**, 3020 (1986).
[61] M. Büttiker, Coherent and sequential tunneling in series barriers, IBM J. Res. Dev. **32**, 63 (1988).
[62] U. Sivan and Y. Imry, Multichannel Landauer formula for thermoelectric transport with application to thermopower near the mobility edge, Phys. Rev. B **33**, 551 (1986).
[63] P. N. Butcher, Thermal and electrical transport formalism for electronic microstructures with many terminals, J. Phys. Condens. Matter **2**, 4869 (1990).
[64] P. Streda, Quantised thermopower of a channel in the ballistic regime, J. Phys. Condens. Matter **1**, 1025 (1989).
[65] L. W. Molenkamp, H. van Houten, C. W. J. Beenakker, R. Eppenga, and C. T. Foxon, Quantum oscillations in the transverse voltage of a channel in the nonlinear transport regime, Phys. Rev. Lett. **65**, 1052 (1990).
[66] G. D. Guttman, E. Ben-Jacob, and D. J. Bergman, Thermopower of mesoscopic and disordered systems, Phys. Rev. B **51**, 17758 (1995).
[67] S. Kheradsoud, N. Dashti, M. Misiorny, P. P. Potts, J. Splettstoesser, and P. Samuelsson, Power, efficiency and fluctuations in a quantum point contact as steady-state thermoelectric heat engine, Entropy **21**, 777 (2019).
[68] G. Haack and F. Giazotto, Efficient and tunable Aharonov-Bohm quantum heat engine, Phys. Rev. B **100**, 235442 (2019).
[69] M. Paulsson and S. Datta, Thermoelectric effect in molecular electronics, Phys. Rev. B **67**, 241403(R) (2003).
[70] P. Reddy, S.-Y. Jang, R. A. Segalman, and A. Majumdar, Thermoelectricity in molecular junctions, Science **315**, 1568 (2007).
[71] D. Sánchez and L. Serra, Thermoelectric transport of mesoscopic conductors coupled to voltage and thermal probes, Phys. Rev. B **84**, 201307(R) (2011).
[72] C. Rangi, H. F. Fotso, H. Terletska, J. Moreno, and K.-M. Tam, Disorder enhanced thermalization in interacting many-particle system, arXiv:2405.13876.
[73] G. Jaliel, R. K. Puddy, R. Sánchez, A. N. Jordan, B. Sothmann, I. Farrer, J. P. Griffiths, D. A. Ritchie, and C. G. Smith, Experimental realization of a quantum dot energy harvester, Phys. Rev. Lett. **123**, 117701 (2019).
[74] T. T. Heikkilä, *The Physics of Nanoelectronics* (Oxford University Press, Oxford, England, 2013).
[75] S. Khandelwal, M. Perarnau-Llobet, S. Seah, N. Brunner, and G. Haack, Characterizing the performance of heat rectifiers, Phys. Rev. Res. **5**, 013129 (2023).
[76] J. L. D'Amato and H. M. Pastawski, Conductance of a disordered linear chain including inelastic scattering events, Phys. Rev. B **41**, 7411 (1990).
[77] M. J. M. de Jong and C. W. J. Beenakker, Semiclassical theory of shot noise in mesoscopic conductors, Physica (Amsterdam) **230A**, 219 (1996).
[78] S. Datta, *Electronic Transport in Mesoscopic Systems* (Cambridge University Press, Cambridge, England, 1995).
[79] S. Bedkihal, M. Bandyopadhyay, and D. Segal, The probe technique far from equilibrium: Magnetic field symmetries of nonlinear transport, Eur. Phys. J. B **86**, 506 (2013).
[80] Y. Utsumi, O. Entin-Wohlman, A. Aharony, T. Kubo, and Y. Tokura, Fluctuation theorem for heat transport probed by a thermal probe electrode, Phys. Rev. B **89**, 205314 (2014).
[81] See Supplemental Material at http://link.aps.org/supplemental/10.1103/PhysRevLett.134.186301 for further information.
[82] P. Roulleau, F. Portier, P. Roche, A. Cavanna, G. Faini, U. Gennser, and D. Mailly, Tuning decoherence with a voltage probe, Phys. Rev. Lett. **102**, 236802 (2009).
[83] H. Haug and A.-P. Jauho, *Quantum Kinetics in Transport and Optics of Semiconductors* (Springer, Berlin, Germany, 2010).
[84] J. P. Bergfield, S. M. Story, R. C. Stafford, and C. A. Stafford, Probing Maxwell's demon with a nanoscale thermometer, ACS Nano **7**, 4429 (2013).
[85] A. Shastry and C. A. Stafford, Temperature and voltage measurement in quantum systems far from equilibrium, Phys. Rev. B **94**, 155433 (2016).
[86] D. Zhang, X. Zheng, and M. Di Ventra, Local temperatures out of equilibrium, Phys. Rep. **830**, 1 (2019).
[87] A. Shastry, S. Inui, and C. A. Stafford, Scanning tunneling thermometry, Phys. Rev. Appl. **13**, 024065 (2020).
[88] L. Tesser, R. S. Whitney, and J. Splettstoesser, Thermodynamic performance of hot-carrier solar cells: A quantum transport model, Phys. Rev. Appl. **19**, 044038 (2023).
[89] A. Braggio, M. Carrega, B. Sothmann, and R. Sánchez, Nonlocal thermoelectric detection of interaction and correlations in edge states, Phys. Rev. Res. **6**, L012049 (2024).
[90] J. R. Prance, C. G. Smith, J. P. Griffiths, S. J. Chorley, D. Anderson, G. A. C. Jones, I. Farrer, and D. A. Ritchie, Electronic refrigeration of a two-dimensional electron gas, Phys. Rev. Lett. **102**, 146602 (2009).
[91] A. A. M. Staring, L. W. Molenkamp, B. W. Alphenaar, H. van Houten, O. J. A. Buyk, M. A. A. Mabesoone, C. W. J. Beenakker, and C. T. Foxon, Coulomb-blockade

oscillations in the thermopower of a quantum dot, Europhys. Lett. **22**, 57 (1993).
[92] A. S. Dzurak, C. G. Smith, C. H. W. Barnes, M. Pepper, L. Martín-Moreno, C. T. Liang, D. A. Ritchie, and G. A. C. Jones, Thermoelectric signature of the excitation spectrum of a quantum dot, Phys. Rev. B **55**, R10197 (1997).
[93] N. Nakpathomkun, H. Q. Xu, and H. Linke, Thermoelectric efficiency at maximum power in low-dimensional systems, Phys. Rev. B **82**, 235428 (2010).
[94] S. F. Svensson, A. I. Persson, E. A. Hoffmann, N. Nakpathomkun, H. A. Nilsson, H. Q. Xu, L. Samuelson, and H. Linke, Lineshape of the thermopower of quantum dots, New J. Phys. **14**, 033041 (2012).
[95] M. Josefsson, A. Svilans, A. M. Burke, E. A. Hoffmann, S. Fahlvik, C. Thelander, M. Leijnse, and H. Linke, A quantum-dot heat engine operating close to the thermodynamic efficiency limits, Nat. Nanotechnol. **13**, 920 (2018).
[96] G. Breit and E. Wigner, Capture of slow neutrons, Phys. Rev. **49**, 519 (1936).
[97] M. Nilsson, L. Namazi, S. Lehmann, M. Leijnse, K. A. Dick, and C. Thelander, Single-electron transport in InAs nanowire quantum dots formed by crystal phase engineering, Phys. Rev. B **93**, 195422 (2016).
[98] D. Barker, S. Lehmann, L. Namazi, M. Nilsson, C. Thelander, K. A. Dick, and V. F. Maisi, Individually addressable double quantum dots formed with nanowire polytypes and identified by epitaxial markers, Appl. Phys. Lett. **114**, 183502 (2019).
[99] A. N. Jordan, B. Sothmann, R. Sánchez, and M. Büttiker, Powerful and efficient energy harvester with resonant-tunneling quantum dots, Phys. Rev. B **87**, 075312 (2013).
[100] B. Szukiewicz, U. Eckern, and K. I. Wysokiński, Optimisation of a three-terminal nonlinear heat nano-engine, New J. Phys. **18**, 023050 (2016).
[101] J. Balduque and R. Sánchez, Coherent control of thermoelectric currents and noise in quantum thermocouples, Phys. Rev. B **109**, 045429 (2024).
[102] I. B. Levinson, Potential distribution in a quantum point contact, Sov. Phys. JETP **68**, 1257 (1989) [Zh. Eksp. Teor. Fiz. **95**, 2175 (1989)], http://www.jetp.ras.ru/cgi-bin/e/index/e/68/6/p1257?a=list.
[103] M. Buttiker, Capacitance, admittance, and rectification properties of small conductors, J. Phys. Condens. Matter **5**, 9361 (1993).
[104] D. Sánchez, R. Sánchez, R. López, and B. Sothmann, Nonlinear chiral refrigerators, Phys. Rev. B **99**, 245304 (2019).
[105] L. P. Kouwenhoven, C. M. Marcus, P. L. McEuen, S. Tarucha, R. M. Westervelt, and N. S. Wingreen, Electron transport in quantum dots, in *Mesoscopic Electron Transport*, edited by L. L. Sohn, L. P. Kouwenhoven, and G. Schön (Springer Netherlands, Dordrecht, 1997), pp. 105–214.
[106] G. Marchegiani, A. Braggio, and F. Giazotto, Nonlinear thermoelectricity with electron-hole symmetric systems, Phys. Rev. Lett. **124**, 106801 (2020).
[107] G. Germanese, F. Paolucci, G. Marchegiani, A. Braggio, and F. Giazotto, Bipolar thermoelectric Josephson engine, Nat. Nanotechnol. **17**, 1084 (2022).
[108] S. Battisti, G. De Simoni, L. Chirolli, A. Braggio, and F. Giazotto, Bipolar thermoelectric superconducting single-electron transistor, Phys. Rev. Res. **6**, L012022 (2024).